12-1-2021

OGR1-dependent regulation of the allergen-induced asthma phenotype

Ajay P Nayak
Thomas Jefferson University

Deepak A. Deshpande, PhD
Thomas Jefferson University

Sushrut D. Shah
Thomas Jefferson University

Dominic R Villalba
Thomas Jefferson University

Roslyn Yi
Thomas Jefferson University

OGR1-dependent regulation of the allergen-induced asthma phenotype

Ajay P. Nayak[1], Deepak A. Deshpande[1], Sushrut D. Shah[1], Dominic R. Villalba[1], Roslyn Yi[1], Nadan Wang[1], Raymond B. Penn[1]

[1]Department of Medicine, Center for Translational Medicine and Division of Pulmonary, Allergy and Critical Care Medicine; Jane & Leonard Korman Lung Center, Thomas Jefferson University, Philadelphia, PA 19107

To whom the correspondence should be addressed: Raymond B. Penn, Center for Translational Medicine, Thomas Jefferson University, Rm 543 JAH, 1020 Locust St., Philadelphia, PA, 19107, Phone: 215-955-9982; Fax: 215-503-5731; Email: raymond.penn@jefferson.edu

Running head: OGR1 regulation of the asthma phenotype

ORCID: **Ajay P. Nayak (0000-0003-3437-0096)**

ABSTRACT

The proton-sensing receptor, ovarian cancer G protein-coupled receptor (OGR1) has been shown to be expressed in airway smooth muscle (ASM) cells and capable of promoting ASM contraction in response to decreased extracellular pH. OGR1 knockout mice (OGR1KO) are reported to be resistant to asthma features induced by inhaled allergen. We recently described certain benzodiazepines as OGR1 activators capable of mediating both pro-contractile and pro-relaxant signaling in ASM cells. Here we assess the effect of treatment with the benzodiazepines lorazepam or sulazepam on the asthma phenotype, in wild type (WT) and OGR1KO mice subjected to inhaled house dust mite (HDM; *Dermatophagoides pteronyssius*) challenge for three weeks. In contrast to previously published reports, both WT and OGR1KO mice developed significant allergen-induced lung inflammation and airway hyperresponsiveness (AHR). In WT mice, treatment with sulazepam (a Gs-biased OGR1 agonist), but not lorazepam (a balanced OGR1 agonist), prevented allergen-induced AHR, although neither drug inhibited lung inflammation. The protection from development of AHR conferred by sulazepam was absent in OGR1KO mice. Treatment of WT mice with sulazepam also resulted in significant inhibition of HDM-induced collagen accumulation in the lung tissue. These findings suggest OGR1 expression is not a requirement for development of the allergen-induced asthma phenotype, but OGR1 can be targeted by the Gs-biased OGR1 agonist sulazepam (but not the balanced agonist lorazepam) to protect from allergen-induced AHR, possibly mediated via suppression of chronic bronchoconstriction and airway remodeling in the absence of effects on airway inflammation.

INTRODUCTION

Asthma is chronic inflammatory disease that is marked with airway inflammation, excessive airway mucus secretion, hyperresponsiveness and remodeling (1). The disease continues to be one of the principal drivers of respiratory morbidity and mortality affecting over 300 million people globally with more than 250,000 deaths annually (2, 3). β-agonists, which activate the G protein-coupled receptor (GPCR) β_2-adrenoceptor (β_2AR), are the principal bronchorelaxant drugs for management of acute asthmatic attacks and are also used in combination with inhaled corticosteroids for prophylactic asthma management. However, concerns regarding β-agonist efficacy (up to 50% of asthmatics experience suboptimal control (4)), as well as safety concerns (5) have stimulated the pursuit of new, superior asthma drugs (6). Recent studies have identified numerous (previously unappreciated) GPCRs in the lung and ASM, such as the calcium sensing receptor (7), bitter tastant receptors (8), and opsin receptors (9, 10) whose targeting might constitute an effective asthma management strategy.

We have identified one such GPCR, the proton-sensing receptor ovarian cancer G-protein coupled receptor (OGR1, *aka* GPR68), whose activation by low extracellular pH causes contraction of human ASM cells (11). Moreover, OGR1 knockout (OGR1KO) mice were reported to be resistant to asthma features induced by inhaled ovalbumin, suggesting OGR1 plays an important role in asthma pathogenesis (12). Therefore, pharmacological targeting of OGR1 is an attractive approach to mitigate features of asthma. Although the study of OGR1 and other proton-sensing GPCRs has been confounded by the rather promiscuous proton being the cognate ligand for these receptors, we recently characterized

certain benzodiazepines, known more commonly as agonists of γ-aminobutyric acid type A ($GABA_A$) receptors in the brain, as activators of OGR1 (13). Moreover, we demonstrated pleiotropic signaling and regulation of OGR1-dependent functions that could be differentially activated depending on the specific benzodiazepine (14, 15). The benzodiazepine lorazepam exhibited the ability to promote both OGR1-dependent pro-contractile (calcium mobilization) and pro-relaxant (cAMP accumulation, PKA activation) signaling, which was associated with no significant regulation of human ASM cell contraction. Further, OGR1-dependent signaling induced by the benzodiazepine sulazepam was limited to cAMP accumulation and PKA activation, which was associated with a relaxation of human ASM cells. Thus, based on the selective activation of the cAMP-PKA pathway, sulazepam can be characterized as a Gs-biased OGR1 agonist, whereas lorazepam represents a balanced ligand activating both Gq and Gs pathways (15).

In the present study, we tested the ability of lorazepam and sulazepam to regulate asthma features in a murine model of allergic lung inflammation. The dependence of benzodiazepine effects on OGR1 was also assessed by comparing effects in wild type (WT) versus OGR1KO mice.

MATERIALS & METHODS

Chemicals and reagents

Lorazepam was purchased from Sigma (St. Louis, MO), and sulazepam was purchased from Specs (Delft, The Netherlands). House dust mite extract (*Dermatophagoides pteronyssinus; Der p*) was purchased from Greer Labs (Lenoir, NC). Alexa Fluor®-488 conjugated secondary antibodies for immunofluorescence studies were obtained from Life Technologies (Carlsbad, CA). Sircol collagen assay kit was purchased from Biocolor Life Sciences (Carrickfergus, UK). Hematoxylin and eosin (H&E) staining kit was purchased from Vector Laboratories (Burlingame, CA). Periodic acid-Schiff (PAS) staining kit was obtained from Sigma. Acid fuchsin orange G (AFOG) stain was prepared by our laboratory.

Murine model of allergic asthma

All animal procedures were approved by the Institutional Animal Care Committee of Thomas Jefferson University, Philadelphia, PA. All methods were performed in accordance with the guidelines and regulations of the institution.

Male and female wild type C57BL/6 mice (8-10 weeks old) and age-matched OGR1KO mice (C57BL/6 background) developed previously (16) were intranasally challenged five days a week for three consecutive weeks with 25 µg of HDM extract in 35 µl phosphate buffered-saline (PBS) (**Figure 1**). A subset of mice was also administered with either lorazepam (3 mg/kg), sulazepam (3.2 mg/kg) or vehicle (10% v/v DMSO) in 25 µl volume via intranasal route ~30 min prior to HDM challenge. Choice of drug dose was based on:1) drug solubility; 2) our previous cell-based studies (11, 14,

15) that demonstrate micromolar concentrations of lorazepam and sulazepam to maximally activate OGR1 in ASM; and 3) the desire to limit systemic/off-target effect of the drugs. Whereas administration of both drugs was followed by a brief period of lethargy in mice, we did not observe any mortality, morbidity, or overt signs suggestive of untoward systemic effects. Aerosol challenges in animals were performed under isoflurane (2-5%) anesthesia. Effects of acute administration of lorazepam or sulazepam in the sensitization model were not tested. Twenty-four hours following the final challenge, lung function measurements were performed, followed by collection of bronchoalveolar lavage (BAL) fluid by perfusing the lungs with 500 µl ice-cold PBS. At the end of the experiment, lungs were filled with 10% formalin and harvested, or fresh lung tissues were frozen in liquid nitrogen for histopathological and biochemical analyses.

Measurement of lung mechanics

Lung mechanics were measured using a flexiVent system (Scireq, Montreal, Canada) using methods described previously (8, 17). Animal surgeries were performed under tribromoethanol (Avertin, 250 mg/kg) anesthesia. Briefly, mice were anesthetized with tribromoethanol and the trachea was intubated with a cannula. Mice were ventilated with a tidal volume of 250 µl at 150 breaths/min. A computer-controlled positive and excitatory pressure (PEEP) of 3 cm H_2O was used for all studies. For data acquisition, mice were subjected to increasing doses of nebulized methacholine (MCh) using a standardized protocol and low frequency forced oscillation technique. Airway resistance (R) was calculated based on

fitting the respiratory mechanical input impedance (Zrs) derived from displacement of ventilator's piston and the pressure in the cylinder to the constant phase model normalized to mouse body weight.

Assessment of bronchoalveolar (BAL) cellularity

Following lung function measurements, BAL fluid was collected from tracheotomized mice as described above. BAL samples were centrifuged at 2000 rpm for 3 min and cell pellet resuspended in 1 ml Roswell Park Memorial Institute medium (containing 5% fetal bovine serum). Total cell count in BAL samples was determined by hemocytometer and data expressed as cells/ml. The BAL cells were pelleted onto microscopic slides and subsequently stained with Hema-3 staining kit (Fisher Scientific, Hampton, NH) and differential cell count was determined using a brightfield microscope.

Assessment of BAL cytokine and chemokine profiles

A panel of cytokines and chemokines were measured in BAL fluid by Multiplex LASER Bead Technology (Eve Technologies, Calgary, Canada) using a 31-Plex mouse cytokine/chemokine array (Cat. # MD31). The concentration of each cytokine was determined by extrapolation from a standard curve and expressed as pg/ml.

Histopathological evaluation of lung tissue

Paraffin embedded tissues were used for histological evaluation as described previously (17) using 5 µm sections mounted on Superfrost™ Plus slides. The lung tissues fixed in 10% formalin were embedded in paraffin, cut and stained with hematoxylin and eosin (H&E), acid fuchsin orange G (AFOG) and periodic-acid Schiff (PAS) using a standard histological protocol. Image acquisition was performed using a brightfield microscope. Airway wall thickness was graded on a scale of 0–3 with 0, no change; 1, mild; 2, moderate; and 3, severe. Scores were reported following blinded and independent evaluation of AFOG-stained tissue sections by two investigators.

Immunofluorescence based detection of smooth muscle α-actin was conducted using methods described previously (17). Slides were deparaffinized, rehydrated and subjected to heat-induced epitope retrieval. The sections after blocking were stained with the primary antibody (1:100 anti-sm-α-actin) at 4°C overnight followed by staining with 1:250 goat anti-mouse Alexa Fluor® conjugated secondary antibody at room temperature for 1 hour. The sections were washed in PBS and stained with Draq5 for 15 min. Finally, the sections were washed, mounted with Prolong Antifade (Molecular Probes, Eugene, OR), and fluorescent imaging performed using an Olympus BX-51 fluorescent microscope. Quantitative estimation of peribronchial sm-α-actin staining was performed using Image J and reported as the ratio of integrated intensity of sm-α-actin staining to peribronchial area.

Preparation of lung tissue protein lysates

Murine lung lobes were excised, cut into small pieces and suspended in 250 µl RIPA lysis buffer (Cell Signaling Technology, Danvers, MA) containing protease and phosphatase inhibitors (Bimake, Houston, TX). Lung tissues were homogenized using a hand-held homogenizer. The lysate was centrifuged (1000 x *g*, 10 min) and the supernatant was stored at -80°C for further analysis.

Immunoblotting

Protein concentration of lung tissue lysates was determined using Pierce BCA Assay kit (Thermo Scientific, Rockford, IL) and subjected to immunoblot analysis using standard methodologies. Blots were probed with primary antibodies to smooth muscle myosin heavy chain (sm MHC) (1:1500) (AbCam, Cambridge, MA), smooth muscle alpha actin (sm α-actin) (1:1000) (AbCam) and β-actin (1:100,000) (Sigma). IRDye-conjugated anti-mouse and anti-rabbit secondary antibodies (LI-COR Biosciences, Lincoln, NE) (1:15,000) were applied to the blots as secondary antibodies. Immunoblots were scanned and immunoreactive bands quantified using the Odyssey® infrared imaging system and software (LI-COR Biosciences).

Soluble collagen assay

Soluble collagen (resulting from active inflammation) was measured in lung lysates obtained from murine lung using Sircol Soluble Collagen Assay (Biocolor, UK) according to the manufacturer's protocol and as described previously (18). This

assay allows for quantitative estimation of acid- and pepsin-soluble collagen species. Lung lysate was mixed with Sircol Dye Reagent allowing collagen to bind to the dye and precipitate. After acid-salt wash, alkali reagent was used to release collagen bound dye into solution and absorbance was measured at 550 nm. A standard curve was established using reference standards provided in the assay kit.

Statistical analysis of data sets

All data sets are represented as mean values ± standard error of means (SEM). The statistical significance was determined using one-way or two-way ANOVA with Bonferroni's post-hoc multiple comparisons test, with $p < 0.05$ being sufficient to establish significant difference between groups. All statistical analyses were performed using Prism8 software (GraphPad, San Diego, CA).

RESULTS

Sulazepam but not lorazepam modulates HDM-induced airway hyperreactivity in mice in an OGR1-dependent manner. Repeated treatment of mice (WT, OGR1KO) with benzodiazepines (lorazepam or sulazepam; PBS treatment serving a control), in conjunction with PBS or HDM treatment, did not adversely affect their growth and mice exhibited no apparent changes in health or behavior. Following cessation of the dosing schedule after 3 weeks, mice were anesthetized to assess changes in airway resistance in response to MCh challenge. Repeated challenge of WT mice with HDM for 3 weeks increased the airway resistance in response to increasing doses of MCh (6.125-25 mg/ml) compared to PBS-challenged animals (**Figure 2A**). OGR1KO mice undergoing HDM treatment demonstrated a similar increase in AHR (**Figure 2B**). Concomitant treatment with lorazepam failed to inhibit the development of AHR in both WT and OGR1KO mice. In contrast, sulazepam treatment significantly ($p<0.05$) inhibited the development of AHR in WT mice, but not in OGR1KO mice. These data suggest that sulazepam can effectively inhibit development of increased airway resistance in a murine model of allergen-induced asthma. However, sulazepam treatment did not protect against development of HDM-induced AHR in OGR1KO mice suggesting the effect of sulazepam is mediated via OGR1.

Lorazepam and sulazepam do not mitigate HDM-induced allergic airway inflammation in mice. Given that allergen-induced AHR was inhibited in mice by treatment with sulazepam in an OGR1-dependent manner, we next sought to determine the mechanism(s) underlying this effect. First, we examined if treatment with benzodiazepines and particularly

sulazepam had any effect on HDM-induced airway inflammation. In WT and OGR1KO mice challenged repeatedly with HDM for 3 weeks, a comparable increase in BAL cellularity was observed (**Figure 3**). In WT mice **(Figure 3A)**, following treatment with lorazepam and sulazepam, the total cellular influx in airways was not reduced and similar trends were noted for the number of lymphocytes and eosinophils in the BAL fluid. Treatment of OGR1KO mice with either benzodiazepine did not inhibit the total cellular influx in the airways resulting from HDM challenge **(Figure 3B)**. Somewhat surprisingly, treatment of OGR1KO mice with sulazepam significantly increased HDM-induced accumulation of eosinophils in BAL fluid. Finally, treatment of WT or OGR1KO mice with either benzodiazepine had no significant effect on levels of eotaxin-1, IL-4, IL-6, IP-10, Cxcl1 and LIF induced by HDM challenge and recovered in the BAL fluid (**Figure 4**). For all other cytokines measured using the multiplex system, the levels were below the threshold of detection (data not shown). Collectively, these data indicate benzodiazepines lack any mitigating effect on multiple indices of airway inflammation, suggesting that sulazepam's ability to inhibit AHR development was not mediated via regulation of airway inflammation.

Effect of inhalation of benzodiazepines on allergen-induced lung tissue inflammation and airway remodeling features. Next, we sought to examine if sulazepam or lorazepam had any effect on the lung tissue inflammation or histological changes in lung architecture induced by repeated inhalation of HDM. Examination of H&E-stained lung tissue sections from WT and OGR1KO mice that were repeatedly challenged with HDM demonstrated typical histopathological

194 features including pleocellular peribronchial and perivascular inflammation (**Figure 5A**) and mucus cell metaplasia
195 (**Figure 5B**). Consistent with our assessment of lung inflammation evident in BAL fluid, in both WT and OGR1KO mice
196 treatment with sulazepam and lorazepam did not result in any changes in HDM-induced infiltration of immune cells in the
197 lung tissue (**Figure 5A**). Further, treatment with either benzodiazepine failed to inhibit HDM-induced goblet cell metaplasia
198 in either mouse genotype (**Figure 5B**).

199 Next, we examined the effect of lorazepam or sulazepam on features of airway remodeling (AR) induced by HDM
200 challenge (**Figures 6 and 7**). Repeated inhalation of HDM resulted in increased collagen staining along the epithelial
201 basement membrane and overall thickening of the airway wall in lungs from both strains of mice (**Figure 6A**). However,
202 microscopic examination of histological sections from sulazepam-treated WT mice revealed no changes in accumulation
203 of collagen around the airways. Lorazepam treatment had no effect on increased accumulation of collagen in lung by
204 HDM challenge. In OGR1KO mice, we observed accumulation of collagen around airways upon HDM challenge and no
205 changes with lorazepam and sulazepam treatment. Further, AFOG stained slides were scored to estimate the airway wall
206 thickness, which increased in mice following challenge with HDM and was unchanged in mice treated with sulazepam or
207 lorazepam (**Figure 6B**). To quantify the difference in collagen accumulation between the treatment groups, we performed
208 Sircol^{TM} Collagen Assay. In WT mice, we observed that treatment with sulazepam (but not lorazepam) significantly
209 reduced the HDM-induced increase in soluble collagen in lungs (**Figure 6C**). Baseline collagen levels in PBS-treated

OGR1KO lungs were higher, but were not significantly increased by HDM challenge. Further, sulazepam and lorazepam treatment did not modulate soluble collagen levels in OGR1KO mice.

Next, we examined ASM mass by staining for smooth muscle alpha actin (sm α-actin) using an immunofluorescence approach. Sm α-actin increased in animals challenged with HDM and was unchanged in sulazepam- or lorazepam-treated mice (**Figure 7A**). Imaging and quantitative analysis revealed significant increase in peribronchial sm α-actin staining in mice repeatedly challenged with HDM which was unchanged in sulazepam- and lorazepam-treated mice (**Figures 7A and 7B**). To further quantify changes in ASM mass, we examined the effect of HDM challenge and lorazepam/sulazepam treatment on expression of smooth muscle markers, sm α-actin and smooth muscle myosin heavy chain (sm MHC) in murine whole lung lysates. Western blotting and subsequent quantitative analysis revealed no significant changes in expression of sm α-actin and sm MHC in lungs of animals challenged with HDM and those concomitantly treated with sulazepam or lorazepam (**Figures 7C and 7D**).

DISCUSSION

In the present study we report that sulazepam, previously shown to be a Gs-biased agonist of OGR1, can inhibit, in an OGR1-dependent manner, AHR development in a murine model of allergic lung inflammation. Moreover, and in contrast to a previous report (12), OGR1KO is not protective against the development of the allergen-induced asthma phenotype.

OGR1 was originally identified as belonging to a unique subfamily of GPCRs classified as *proton-sensing* GPCRs, based on their ability to signal in response to reduced extracellular pH. Although the ability to study OGR1 to date has been significantly hampered by its cognate ligand being the promiscuous proton, recent discoveries have facilitated research into this receptor. We recently reported the ability of certain benzodiazepines to function as activators of the proton-sensing receptor OGR1 (13), and further demonstrated that OGR1 signaling could be biased, dependent on the specific benzodiazepine employed (15). In Pera *et al*. we established that lorazepam could promote both G_q- and G_s-dependent OGR1 signaling, whereas sulazepam only activated OGR1-mediated G_s-cAMP-PKA signaling. Consistent with ability of G_q and G_s signaling to mediate contraction and relaxation, respectively, of ASM, only sulazepam was found to effect relaxation of ASM cells as assessed by Magnetic Twisting Cytometry (15, 19).

Intrigued by the possibility that sulazepam, by biasing OGR1 signaling to the G_s-PKA pathway, could be an effective anti-asthma drug, we tested the effectiveness of lorazepam and sulazepam in an *in vivo* murine model of asthma using WT and OGR1KO mice. Although both drugs failed to mitigate features of allergen-induced asthma in mice, sulazepam inhibited development of HDM allergen-induced AHR in an OGR1-dependent manner. AHR is largely understood to have

two components; ‘baseline’ (chronic) highlighted by structural alterations, and ‘variable’ which is marked by episodic airway inflammation (20). Sulazepam had no effect on airway inflammation suggesting a lack of effect on ‘variable’ component of AHR development. However, we demonstrate that sulazepam significantly reduced subepithelial collagen accumulation in the lungs, while most of the other features of airway remodeling (such as increased airway mass) were unaffected, indicating an effect on ‘baseline’ or chronic component of AHR development. Previously, multiple studies have suggested that subepithelial deposition of collagen can contribute to the development of AHR (20-25). The inhibitory actions of sulazepam on subepithelial deposition of collagen are also similar to those previously reported for long acting β-agonists (LABAs) (26). Whether a broader effect of sulazepam on indices of airway remodeling could occur in a more chronic model of allergic inflammation, requires further investigation.

Moreover, it has also been suggested that increased ASM contractility is also a mechanical determinant of ‘chronic’ AHR development (27). One possible mechanism by which sulazepam may regulate AHR development is by suppressing chronic ASM contractility. In our model, this would be sustained by daily inhalation of sulazepam prior to challenge with HDM. Previously, we established that sulazepam activates OGR1 in a biased manner to preferentially signal through G_s-cAMP-PKA pathway (15), which can antagonize contractile signaling in ASM cells at multiple junctions (28, 29). This could also partly explain why lorazepam was not as effective in protecting HDM-challenged WT mice from developing AHR, given lorazepam activates both G_q and G_s signaling, whose competing effects could effectively cancel each other out. Moreover, although our previous studies demonstrated that sulazepam could stimulate cAMP/PKA under physiological pH

256 (7.4), sulazepam-stimulated cAMP-PKA was actually higher at lower pH's. Thus, the acidic airway microenvironment
257 shown to exist in the inflamed asthmatic airway (11, 30) likely further augments the cAMP-PKA-mediated ASM relaxant
258 effect of sulazepam.

259 Finally, benzodiazepines have been demonstrated to cause respiratory depression (31, 32). Such respiratory
260 depression could possibly contribute to the observed effects of benzodiazepines on HDM-induced AHR, including
261 exacerbation of the already low pH observed in the asthmatic lung associated with lung inflammation (30). Although such
262 effects of sulazepam have yet to studied, it is possible that sulazepam may act in a similar manner.

263 In a previous study, it was reported that OGR1KO mice were resistant to allergen-induced allergic airway
264 inflammation, partly attributed to the suboptimal migration and function of dendritic cells (12). In the current study, we
265 demonstrate that OGR1KO are susceptible to allergen-induced airway inflammation and demonstrate increased AHR.
266 The choice of allergen (ovalbumin vs HDM) and the strain of mice (BALB/c vs C57BL/6) employed in the two models are
267 different and may account for the conflicting results. Notably, eosinophil numbers were higher in OGR1KO mice treated
268 with sulazepam, suggesting possible off-target effects of sulazepam on the $GABA_A$ receptors or the peripheral
269 benzodiazepine receptor (TSPO; 18 kDa translocator protein).

270 In conclusion, our studies indicate that OGR1 is not a requirement for development of allergen-induced inflammation
271 and the asthma phenotype but can be targeted by the Gs-biased benzodiazepine sulazepam to protect mice from

allergen-induced AHR but not lung inflammation. OGR1-dependent mechanisms effecting this protection may include mitigation of airway remodeling and inhibition of chronic ASM contraction caused by chronic inflammation.

Acknowledgements

This study was funded by National Institutes of Health Heart, Lung, and Blood Institute Grant P01HL114471 (to RBP).

Conflicts of interest

The authors report no conflicts of interest.

REFERENCES

1. Olin JT, Wechsler ME. Asthma: pathogenesis and novel drugs for treatment. *BMJ* 2014; 349: g5517.
2. CDC. CDC Vital Signs: Asthma in the US growing every year. 2011.
3. WHO. Global surveillance, prevention and control of chronic respiratory diseases: a comprehensive approach. 2007.
4. Peters SP, Jones CA, Haselkorn T, Mink DR, Valacer DJ, Weiss ST. Real-world Evaluation of Asthma Control and Treatment (REACT): findings from a national Web-based survey. *J Allergy Clin Immunol* 2007; 119: 1454-1461.
5. Salpeter SR, Wall AJ, Buckley NS. Long-acting beta-agonists with and without inhaled corticosteroids and catastrophic asthma events. *Am J Med* 2010; 123: 322-328 e322.
6. Pera T, Penn RB. Bronchoprotection and bronchorelaxation in asthma: New targets, and new ways to target the old ones. *Pharmacol Ther* 2016; 164: 82-96.
7. Yarova PL, Stewart AL, Sathish V, Britt RD, Jr., Thompson MA, AP PL, Freeman M, Aravamudan B, Kita H, Brennan SC, Schepelmann M, Davies T, Yung S, Cholisoh Z, Kidd EJ, Ford WR, Broadley KJ, Rietdorf K, Chang W, Bin Khayat ME, Ward DT, Corrigan CJ, JP TW, Kemp PJ, Pabelick CM, Prakash YS, Riccardi D. Calcium-sensing receptor antagonists abrogate airway hyperresponsiveness and inflammation in allergic asthma. *Sci Transl Med* 2015; 7: 284ra260.
8. Deshpande DA, Wang WC, McIlmoyle EL, Robinett KS, Schillinger RM, An SS, Sham JS, Liggett SB. Bitter taste receptors on airway smooth muscle bronchodilate by localized calcium signaling and reverse obstruction. *Nat Med* 2010; 16: 1299-1304.
9. Wu AD, Dan W, Zhang Y, Vemaraju S, Upton BA, Lang RA, Buhr ED, Berkowitz DE, Gallos G, Emala CW, Yim PD. Opsin 3-Galphas Promotes Airway Smooth Muscle Relaxation Modulated by G Protein Receptor Kinase 2. *Am J Respir Cell Mol Biol* 2021; 64: 59-68.
10. Yim PD, Gallos G, Perez-Zoghbi JF, Zhang Y, Xu D, Wu A, Berkowitz DE, Emala CW. Airway smooth muscle photorelaxation via opsin receptor activation. *Am J Physiol Lung Cell Mol Physiol* 2019; 316: L82-L93.
11. Saxena H, Deshpande DA, Tiegs BC, Yan H, Battafarano RJ, Burrows WM, Damera G, Panettieri RA, Dubose TD, Jr., An SS, Penn RB. The GPCR OGR1 (GPR68) mediates diverse signalling and contraction of airway smooth muscle in response to small reductions in extracellular pH. *Br J Pharmacol* 2012; 166: 981-990.
12. Aoki H, Mogi C, Hisada T, Nakakura T, Kamide Y, Ichimonji I, Tomura H, Tobo M, Sato K, Tsurumaki H, Dobashi K, Mori T, Harada A, Yamada M, Mori M, Ishizuka T, Okajima F. Proton-sensing ovarian cancer G protein-coupled receptor 1 on dendritic cells is required for airway responses in a murine asthma model. *PLoS One* 2013; 8: e79985.
13. Huang XP, Karpiak J, Kroeze WK, Zhu H, Chen X, Moy SS, Saddoris KA, Nikolova VD, Farrell MS, Wang S, Mangano TJ, Deshpande DA, Jiang A, Penn RB, Jin J, Koller BH, Kenakin T, Shoichet BK, Roth BL. Allosteric ligands for the pharmacologically dark receptors GPR68 and GPR65. *Nature* 2015; 527: 477-483.
14. Nayak AP, Pera T, Deshpande DA, Michael JV, Liberato JR, Pan S, Tompkins E, Morelli HP, Yi R, Wang N, Penn RB. Regulation of ovarian cancer G protein-coupled receptor-1 expression and signaling. *Am J Physiol Lung Cell Mol Physiol* 2019; 316: L894-L902.

15. Pera T, Deshpande DA, Ippolito M, Wang B, Gavrila A, Michael JV, Nayak AP, Tompkins E, Farrell E, Kroeze WK, Roth BL, Panettieri RA, Jr., Benovic JL, An SS, Dulin NO, Penn RB. Biased signaling of the proton-sensing receptor OGR1 by benzodiazepines. *FASEB J* 2018; 32: 862-874.
16. Li H, Wang D, Singh LS, Berk M, Tan H, Zhao Z, Steinmetz R, Kirmani K, Wei G, Xu Y. Abnormalities in osteoclastogenesis and decreased tumorigenesis in mice deficient for ovarian cancer G protein-coupled receptor 1. *PLoS One* 2009; 4: e5705.
17. Sharma P, Yi R, Nayak AP, Wang N, Tang F, Knight MJ, Pan S, Oliver B, Deshpande DA. Bitter Taste Receptor Agonists Mitigate Features of Allergic Asthma in Mice. *Sci Rep* 2017; 7: 46166.
18. Schaafsma D, Dueck G, Ghavami S, Kroeker A, Mutawe MM, Hauff K, Xu FY, McNeill KD, Unruh H, Hatch GM, Halayko AJ. The mevalonate cascade as a target to suppress extracellular matrix synthesis by human airway smooth muscle. *Am J Respir Cell Mol Biol* 2011; 44: 394-403.
19. An SS, Bai TR, Bates JH, Black JL, Brown RH, Brusasco V, Chitano P, Deng L, Dowell M, Eidelman DH, Fabry B, Fairbank NJ, Ford LE, Fredberg JJ, Gerthoffer WT, Gilbert SH, Gosens R, Gunst SJ, Halayko AJ, Ingram RH, Irvin CG, James AL, Janssen LJ, King GG, Knight DA, Lauzon AM, Lakser OJ, Ludwig MS, Lutchen KR, Maksym GN, Martin JG, Mauad T, McParland BE, Mijailovich SM, Mitchell HW, Mitchell RW, Mitzner W, Murphy TM, Pare PD, Pellegrino R, Sanderson MJ, Schellenberg RR, Seow CY, Silveira PS, Smith PG, Solway J, Stephens NL, Sterk PJ, Stewart AG, Tang DD, Tepper RS, Tran T, Wang L. Airway smooth muscle dynamics: a common pathway of airway obstruction in asthma. *Eur Respir J* 2007; 29: 834-860.
20. Cockcroft DW, Davis BE. Mechanisms of airway hyperresponsiveness. *J Allergy Clin Immunol* 2006; 118: 551-559; quiz 560-551.
21. Boulet LP, Laviolette M, Turcotte H, Cartier A, Dugas M, Malo JL, Boutet M. Bronchial subepithelial fibrosis correlates with airway responsiveness to methacholine. *Chest* 1997; 112: 45-52.
22. Brewster CE, Howarth PH, Djukanovic R, Wilson J, Holgate ST, Roche WR. Myofibroblasts and subepithelial fibrosis in bronchial asthma. *Am J Respir Cell Mol Biol* 1990; 3: 507-511.
23. Chetta A, Foresi A, Del Donno M, Bertorelli G, Pesci A, Olivieri D. Airways remodeling is a distinctive feature of asthma and is related to severity of disease. *Chest* 1997; 111: 852-857.
24. Benayoun L, Druilhe A, Dombret MC, Aubier M, Pretolani M. Airway structural alterations selectively associated with severe asthma. *Am J Respir Crit Care Med* 2003; 167: 1360-1368.
25. Ward C, Pais M, Bish R, Reid D, Feltis B, Johns D, Walters EH. Airway inflammation, basement membrane thickening and bronchial hyperresponsiveness in asthma. *Thorax* 2002; 57: 309-316.
26. Goulet S, Bihl MP, Gambazzi F, Tamm M, Roth M. Opposite effect of corticosteroids and long-acting beta(2)-agonists on serum- and TGF-beta(1)-induced extracellular matrix deposition by primary human lung fibroblasts. *J Cell Physiol* 2007; 210: 167-176.
27. Lauzon AM, Martin JG. Airway hyperresponsiveness; smooth muscle as the principal actor. *F1000Res* 2016; 5.
28. Billington CK, Ojo OO, Penn RB, Ito S. cAMP regulation of airway smooth muscle function. *Pulm Pharmacol Ther* 2013; 26: 112-120.
29. Penn RB, Benovic JL. Regulation of heterotrimeric G protein signaling in airway smooth muscle. *Proc Am Thorac Soc* 2008; 5: 47-57.

30. Ricciardolo FL, Gaston B, Hunt J. Acid stress in the pathology of asthma. *J Allergy Clin Immunol* 2004; 113: 610-619.
31. Vozoris NT. Do benzodiazepines contribute to respiratory problems? *Expert Rev Respir Med* 2014; 8: 661-663.
32. Vozoris NT, Fischer HD, Wang X, Stephenson AL, Gershon AS, Gruneir A, Austin PC, Anderson GM, Bell CM, Gill SS, Rochon PA. Benzodiazepine drug use and adverse respiratory outcomes among older adults with COPD. *Eur Respir J* 2014; 44: 332-340.

Figure Legends

Figure 1: **Allergen sensitization and benzodiazepine treatment schedule.** C57BL/6 mice (8-10 weeks old) and age matched OGR1KO mice (C57BL/6 background) were sensitized to HDM allergen (25 µg) administered intranasally for 5 days/week for 3 weeks. Thirty min prior to sensitization, mice were treated with lorazepam or sulazepam (3 mg/kg) via intranasal instillation. Twenty-hours post final sensitization/treatment; mice were anesthetized for flexiVent analysis and collection of bronchoalveolar lavage fluid (BALF). Following this, lung tissue was harvested from animals for generating histological sections and protein lysates.

Figure 2: **Allergen-induced AHR and effect of prophylactic treatment with benzodiazepines. (A)** WT and **(B)** OGR1KO mice were subjected to increasing doses of nebulized methacholine challenge protocol to study respiratory mechanics. Mean total airway resistance (R_s) was computed for each dose for all animals within treatment groups. Data shown above represent a mean from n=6-12 animals per group (R_{avg} ± SEM; standard error of means). * denotes statistical significance (p<0.05) relative to PBS treated mice and $^{\#}$ denotes statistical significance (p<0.05) between HDM

challenged, vehicle-treated and sulazepam-treated groups. Statistical differences are assessed for magnitude of change in R_s at each concentration of MCh across all treatment groups. Lor: lorazepam, Sul: sulazepam, HDM: house dust mite, PBS: phosphate buffered saline.

Figure 3: **Effect of benzodiazepines on allergen-induced airway inflammation.** BALF total and differential cell counts in **(A)** WT and **(B)** OGR1KO mice. Total BALF cell count was determined using a hemocytometer. Differential staining was used to determine proportions of specific immune cell populations. Data shown above represent mean ± SEM mean from n=6-12 animals per group. * denotes statistical significance (p<0.05) relative to PBS treated mice and # denotes statistical significance (p<0.05) between HDM challenged, vehicle-treated and sulazepam-treated groups. Lor: lorazepam, Sul: sulazepam, HDM: house dust mite, PBS: phosphate buffered saline.

Figure 4: **Effect of benzodiazepines on allergen-induced airway cytokine and chemokine profile.** BALF cytokine and chemokine levels were measured in **(A)** WT and **(B)** OGR1KO mice using Multiplexed LASER bead technology. Data shown above represent mean ± SEM from n = 6-12 animals per group. * denotes statistical significance (p<0.05) relative to PBS treated mice and # denotes statistical significance (p<0.05) between HDM challenged, vehicle-treated and sulazepam-treated groups. Lor: Lorazepam, Sul: Sulazepam, HDM: house dust mite, PBS: phosphate buffered saline, IP-10: interferon-γ-induced protein 10, LIF: leukemia inhibitory factor.

Figure 5: **Histopathological changes in murine lung tissue.** Histopathological analyses were performed on paraffin-embedded lung tissue sections stained with either **(A)** H&E or **(B)** PAS stains. Data represent mean ± SEM values, n = 3-5 mice per group. HDM: house dust mite, PBS: phosphate buffered saline.

Figure 6: **Histological evaluation of collagen deposition and examination of soluble collagen. (A)** Paraffin-embedded lung tissue sections stained with acid fuchsin orange G (AFOG). Collagen deposition around airways is highlighted by black arrows. Bar size: 125 μm. **(B)** Quantification of airway wall thickness in AFOG stained murine lung tissue slides. **(C)** Soluble collagen levels were measured in lung tissue lysates generated from WT and OGR1KO mice challenged with HDM and treated with vehicle or benzodiazepines. * denotes statistical significance (p<0.05) relative to PBS treated mice and $^{\#}$ denotes statistical significance (p<0.05) between HDM challenged, vehicle-treated and sulazepam-treated groups. Lor: Lorazepam, Sul: Sulazepam, HDM: house dust mite, PBS: phosphate buffered saline.

Figure 7: **Immunofluorescence and western blot analysis of airway remodeling markers. (A)** Immunofluorescence staining of smooth muscle alpha-actin (sm α-actin). Positive staining for sm α-actin (green) is highlighted by yellow arrows. Bar size: 50 μm. **(B)** Quantification of peribronchial sm α-actin staining. * denotes statistical significance (p<0.05) relative to PBS treated mice and $^{\#}$ denotes statistical significance (p<0.05) between HDM challenged, vehicle-treated and

sulazepam-treated groups. **(C)** Western blot analysis and **(D)** Quantitative estimation of sm MHC and sm α-actin levels in murine lung lysates. Data represented as mean integrated signal intensity for sm MHC or sm α-actin normalized to integrated signal intensity of β-actin. Data represent mean ± SEM values, n = 3-6 mice per group. PBS: phosphate buffered saline, HDM: house dust mite, Lor: lorazepam, Sul: sulazepam, sm: smooth muscle, MHC: myosin heavy chain.

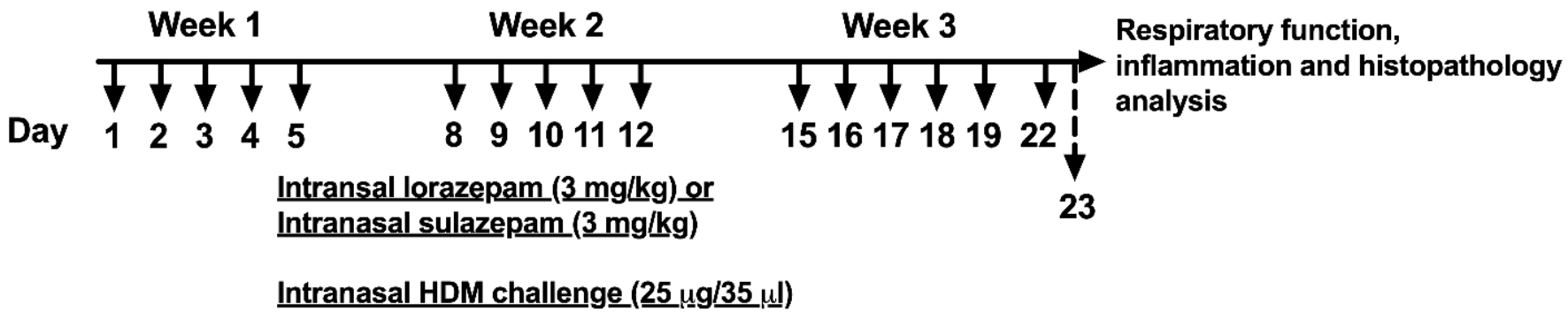
Week 1
Week 2
Week 3
Respiratory function, inflammation and histopathology analysis
Day
1 2 3 4 5 8 9 10 11 12 15 16 17 18 19 22
23
Intransal lorazepam (3 mg/kg) or
Intranasal sulazepam (3 mg/kg)
Intranasal HDM challenge (25 μg/35 μl)

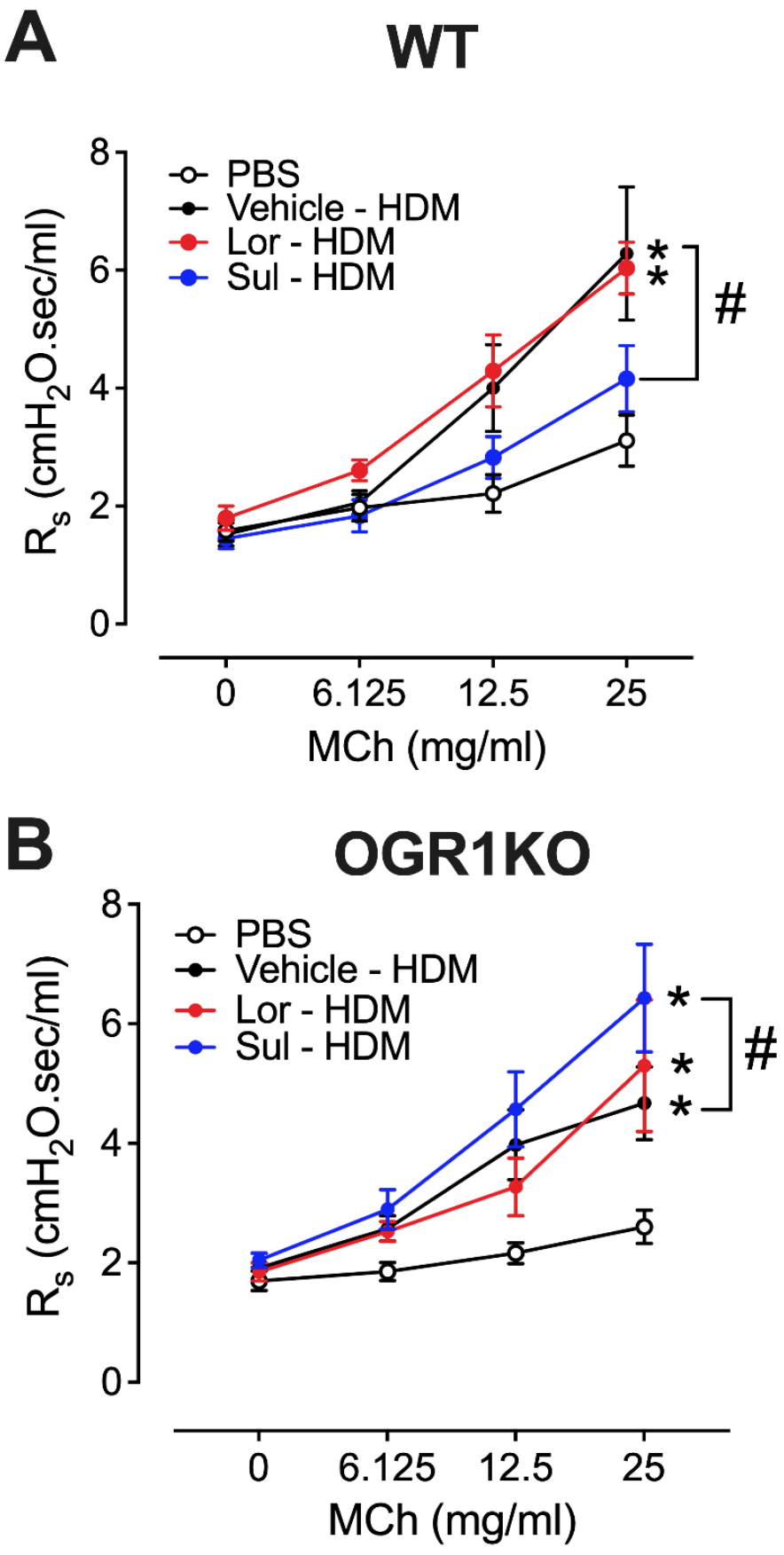
A
WT
PBS
Vehicle - HDM
Lor - HDM
Sul - HDM
R_s (cmH_2O.sec/ml)
0
2
4
6
8
0
6.125
12.5
25
MCh (mg/ml)
**
#
B
OGR1KO
PBS
Vehicle - HDM
Lor - HDM
Sul - HDM
R_s (cmH_2O.sec/ml)
0
2
4
6
8
0
6.125
12.5
25
MCh (mg/ml)
*
*
*
#

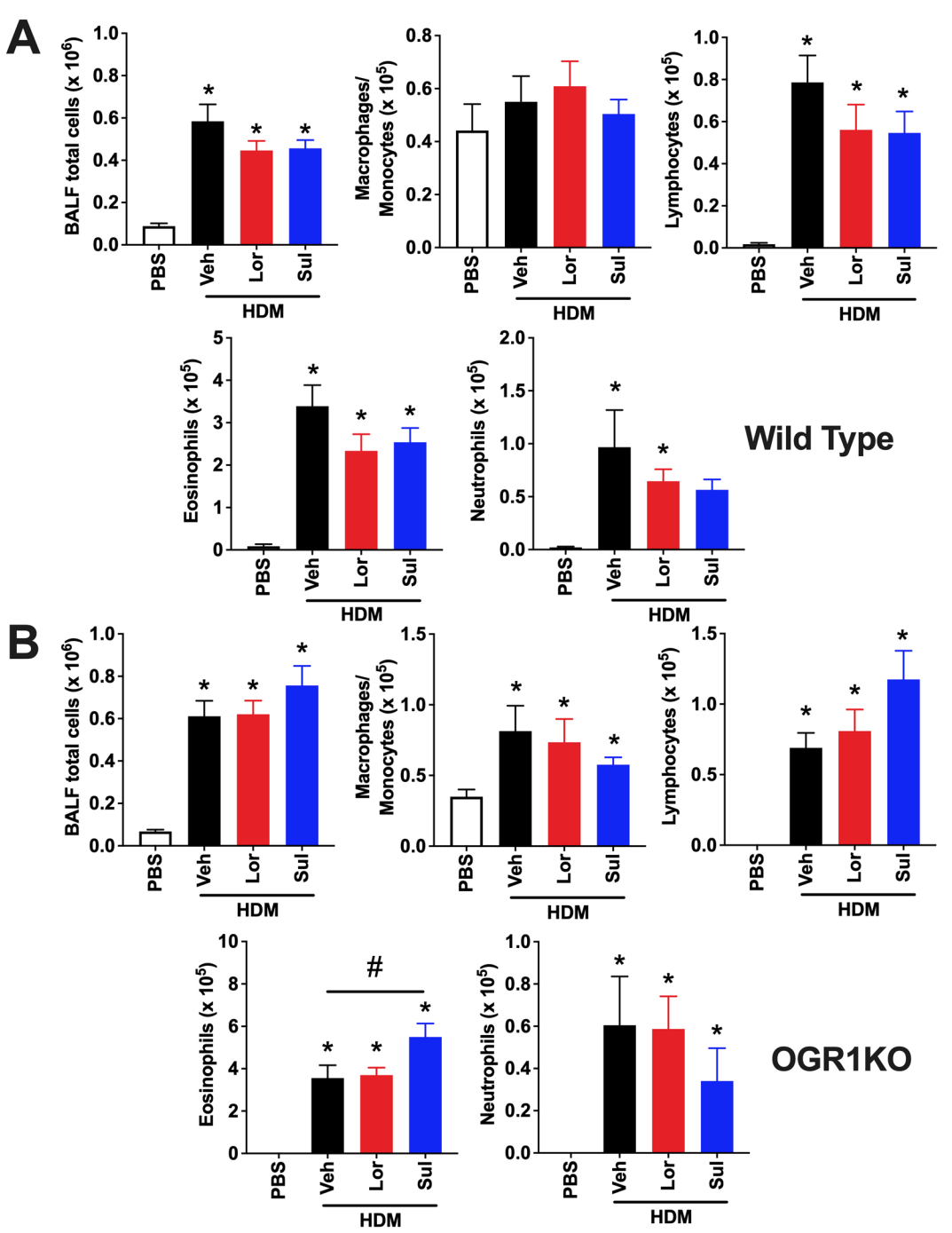
A
BALF total cells (x 10^6)
Macrophages/ Monocytes (x 10^5)
Lymphocytes (x 10^5)
Eosinophils (x 10^5)
Neutrophils (x 10^5)
PBS
Veh
Lor
Sul
HDM
Wild Type
B
BALF total cells (x 10^6)
Macrophages/ Monocytes (x 10^5)
Lymphocytes (x 10^5)
Eosinophils (x 10^5)
Neutrophils (x 10^5)
#
OGR1KO

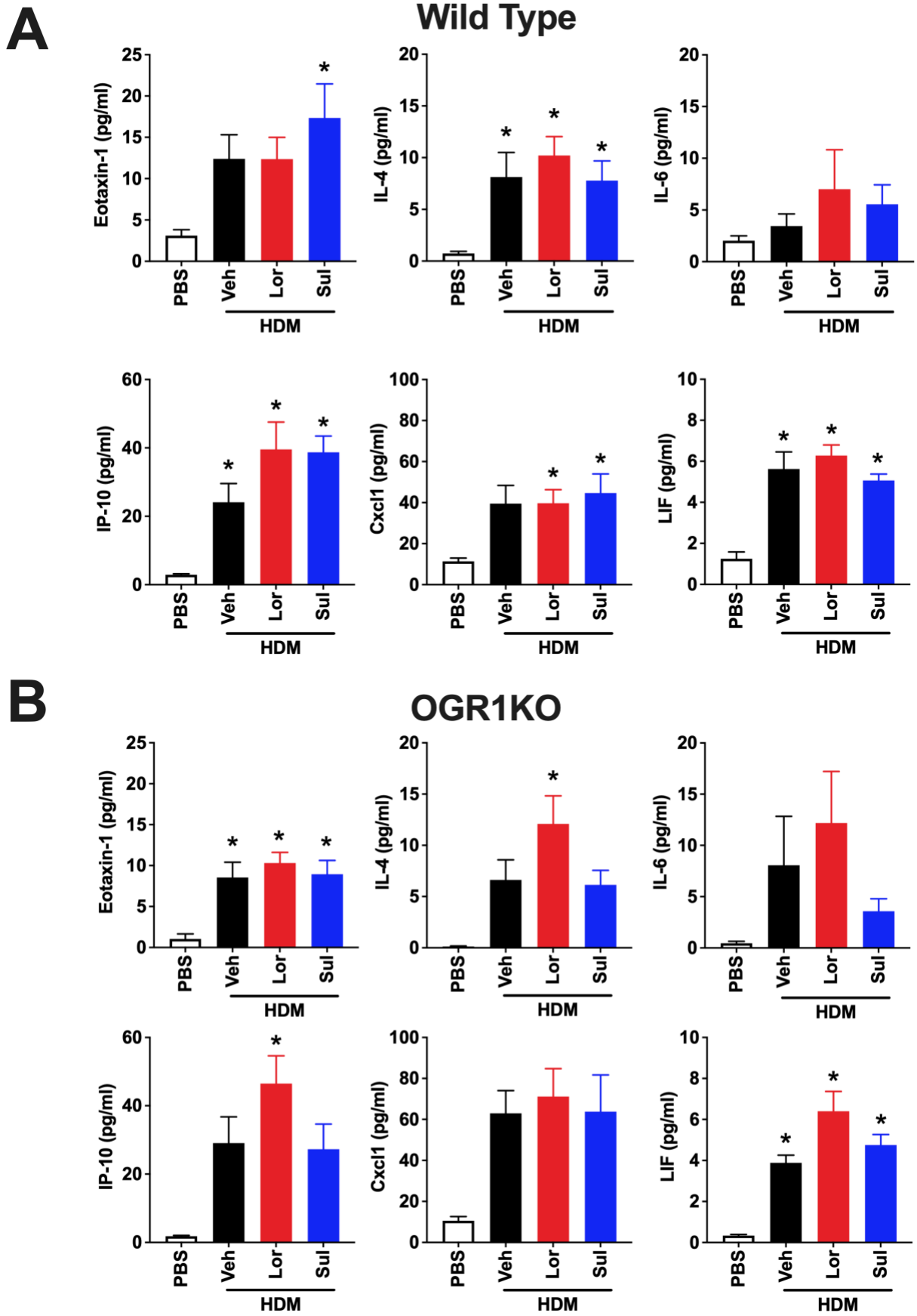
A
Wild Type
Eotaxin-1 (pg/ml)
IL-4 (pg/ml)
IL-6 (pg/ml)
IP-10 (pg/ml)
Cxcl1 (pg/ml)
LIF (pg/ml)
PBS
Veh
Lor
Sul
HDM
B
OGR1KO
Eotaxin-1 (pg/ml)
IL-4 (pg/ml)
IL-6 (pg/ml)
IP-10 (pg/ml)
Cxcl1 (pg/ml)
LIF (pg/ml)
PBS
Veh
Lor
Sul
HDM

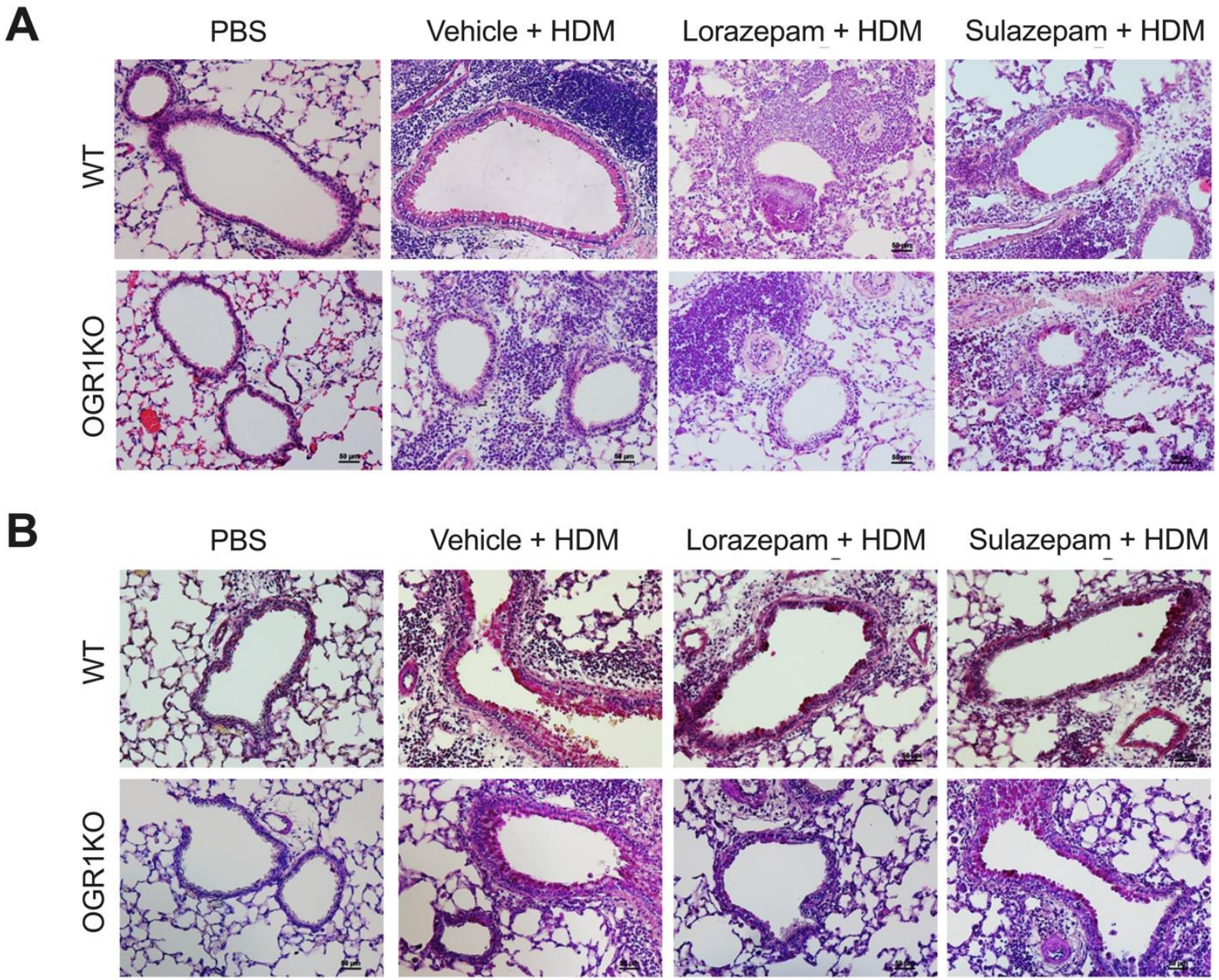
A
PBS
Vehicle + HDM
Lorazepam + HDM
Sulazepam + HDM
WT
OGR1KO
B
PBS
Vehicle + HDM
Lorazepam + HDM
Sulazepam + HDM
WT
OGR1KO

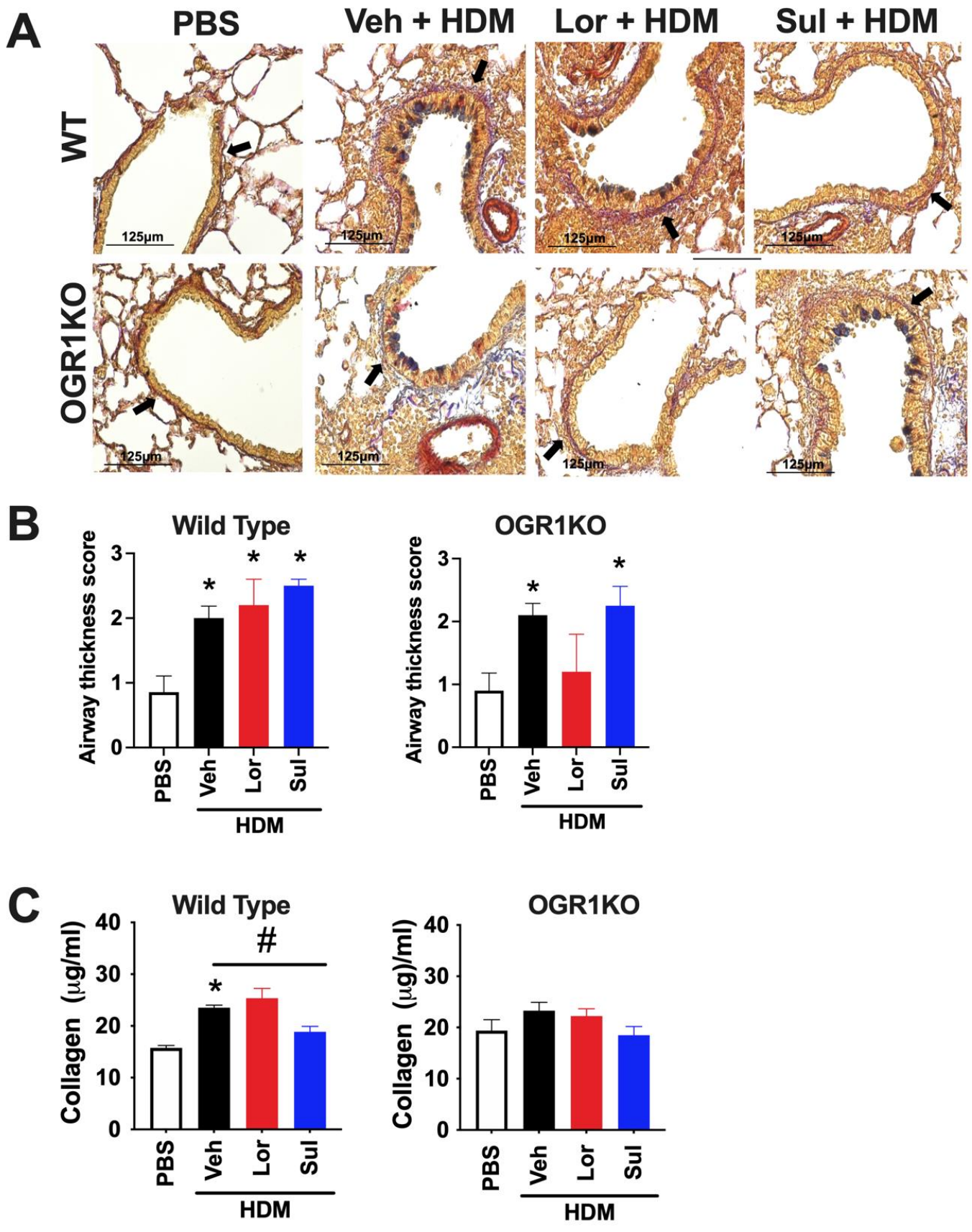
A
PBS
Veh + HDM
Lor + HDM
Sul + HDM
WT
OGR1KO
125μm
B
Wild Type
OGR1KO
Airway thickness score
PBS
Veh
Lor
Sul
HDM
C
Wild Type
OGR1KO
Collagen (μg/ml)
#

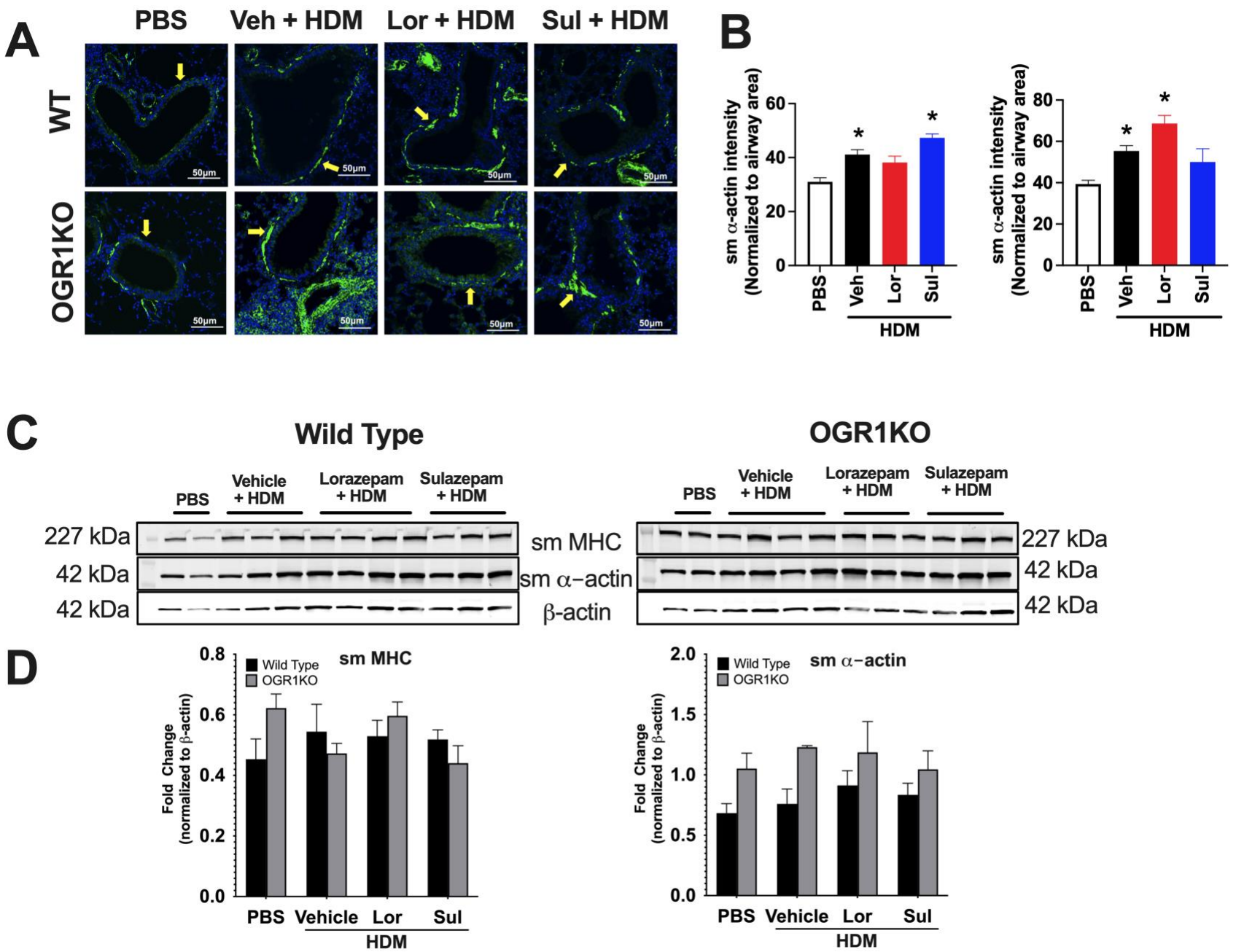
A
PBS
Veh + HDM
Lor + HDM
Sul + HDM
WT
OGR1KO
50μm
B
sm α-actin intensity
(Normalized to airway area)
PBS
Veh
Lor
Sul
HDM
C
Wild Type
OGR1KO
PBS
Vehicle + HDM
Lorazepam + HDM
Sulazepam + HDM
227 kDa
42 kDa
42 kDa
sm MHC
sm α−actin
β-actin
D
sm MHC
sm α−actin
Wild Type
OGR1KO
Fold Change
(normalized to β-actin)
PBS
Vehicle
Lor
Sul
HDM